ADVANCED MATERIALS

Supporting Information

for *Adv. Mater.,* DOI: 10.1002/adma.202202992

Microstructured Hydrogels to Guide Self-Assembly and Function of Lung Alveolospheres

Claudia Loebel, Aaron I. Weiner, Madeline K. Eiken, Jeremy B. Katzen, Michael P. Morley, Vikram Bala, Fabian L. Cardenas-Diaz, Matthew D. Davidson, Kazushige Shiraishi, Maria C. Basil, Laura T. Ferguson, Jason R. Spence, Matthias Ochs, Michael F. Beers, Edward E. Morrisey, Andrew E. Vaughan, and Jason A. Burdick**

WILEY-VCH

Supporting Information

Microstructured hydrogels to guide self-assembly and function of lung alveolospheres

Claudia Loebel, Aaron I. Weiner, Madeline K. Eiken, Jeremy B. Katzen, Michael P. Morley, Vikram Bala, Fabian L. Cardenas-Diaz, Matthew D. Davidson, Kazushige Shiraishi, Maria C. Basil, Laura T. Ferguson, Jason R. Spence, Matthias Ochs, Michael F. Beers, Edward E. Morrisey, Andrew E. Vaughan, and Jason A. Burdick**

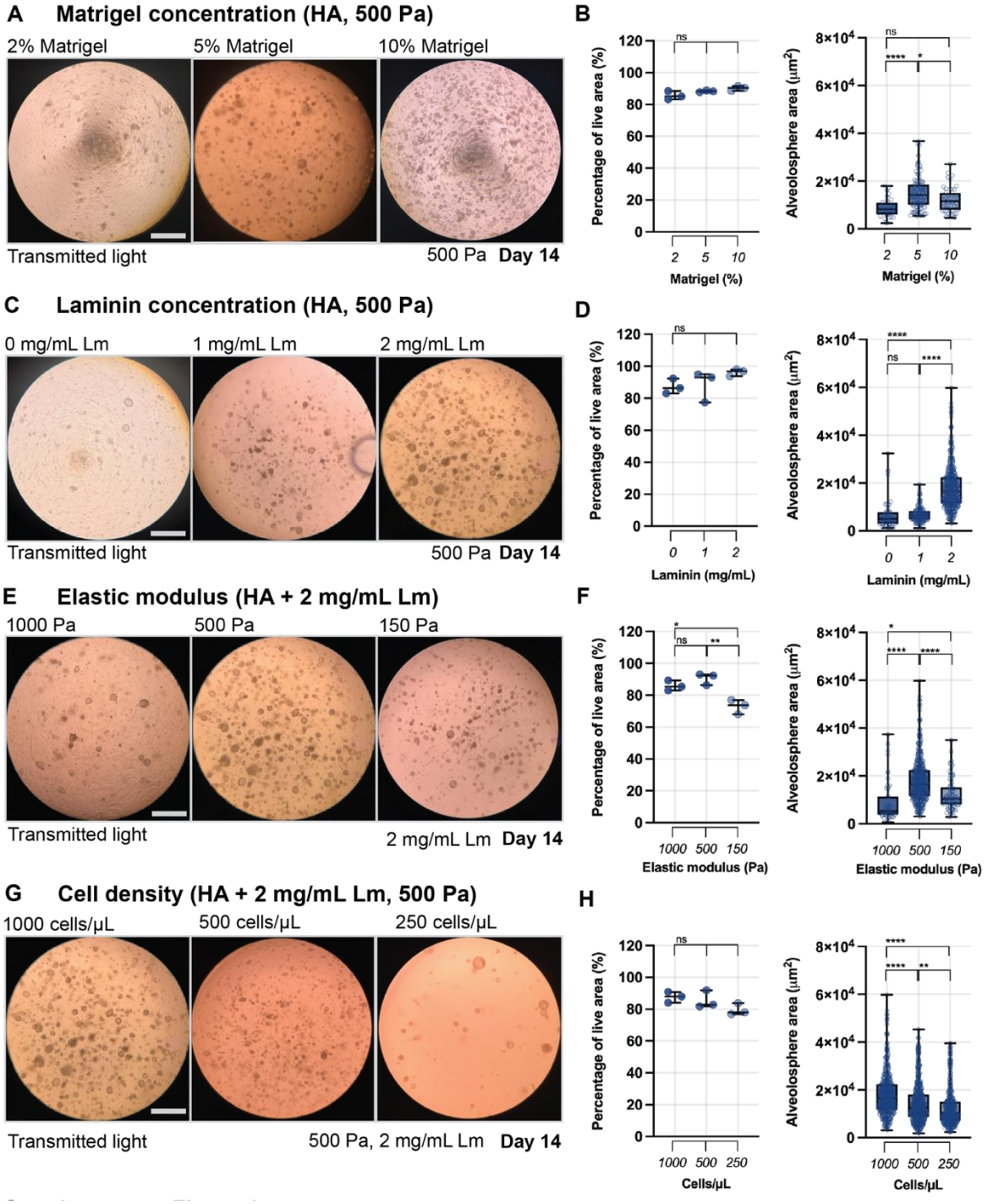

Supplementary Figure 1: Influence of hyaluronic acid hydrogel composition, modulus and seeding density on viability and growth of alveolospheres.

A Representative images of alveolospheres formed in hyaluronic acid hydrogels containing Matrigel (2%, 5% and 10% (vol/vol)) at 14 days (G' 500 Pa with a seeding density of 1000 iAT2s/μL).

B Quantification of percentage of live area (quantified by Calcein AM (live cells) and Ethidium homodimer (dead cells) staining) and the projected area of alveolospheres at 14 days in culture (****p<0.0001, *p<0.05, ns = not significantly different by ANOVA and Bonferroni's multiple comparisons test, live area averaged from 3 independent experiments, n = 32 (2%), 106 (5%), 48 (10%)).

C Representative images of alveolospheres formed in hyaluronic acid hydrogels containing laminin/entactin (0 mg/mL, 1 mg/mL, 2 mg/mL) at 14 days (G' 500 Pa with a seeding density of 1000 iAT2s/µL).
D Quantification of percentage of live area (quantified by Calcein AM (live cells) and Ethidium homodimer (dead cells) staining) and the projected area of alveolospheres at 14 days in culture (****p<0.0001, ns = not significantly different by ANOVA and Bonferroni's multiple comparisons test, live area averaged from 3 independent experiments, n = 55 (0 mg/mL), 165 (1 mg/mL), 430 (2 mg/mL)).
E Representative images of alveolospheres formed in hyaluronic acid hydrogels of different initial modulus (1000 Pa, 500 Pa, 150 Pa) at 14 days (2 mg/mL laminin/entactin with a seeding density of 1000 iAT2s/µL).
F Quantification of percentage of live area (quantified by Calcein AM (live cells) and Ethidium homodimer (dead cells) staining) and the projected area of alveolospheres at 14 days in culture (****p<0.0001, **p<0.01, *p<0.05, ns = not significantly different by ANOVA and Bonferroni's multiple comparisons test, live area averaged from 3 independent experiments, n = 53 (1000 Pa), 430 (500 Pa), 90 (150 Pa)).
G Representative images of alveolospheres formed in hyaluronic acid hydrogels with different cell seeding densities (1000 cells/µL, 500 cells/µL, 250 cells/µL) at 14 days (G' 500 Pa with 2 mg/mL laminin/entactin).
H Quantification of percentage of live area (quantified by Calcein AM (live cells) and Ethidium homodimer (dead cells) staining) and the projected area of alveolospheres at 14 days in culture (****p<0.0001, **p<0.01, ns = not significantly different by ANOVA and Bonferroni's multiple comparisons test, live area averaged from 3 independent experiments, n = 434 (1000 cells/µL), 630 (500 cells/µL), 410 (250 cells/µL)).

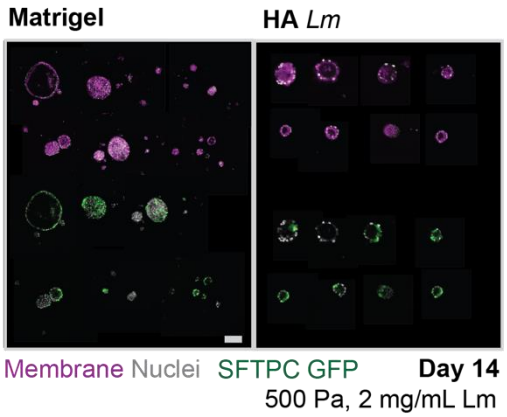

Supplementary Figure 2: Expression of SFTPC^{GFP+} in alveolospheres formed in Matrigel and hyaluronic acid hydrogels with 2 mg/mL laminin/entactin
Representative images of SFTPC^{GFP+} alveolospheres formed in Matrigel and hyaluronic acid hydrogels with 2 mg/mL laminin/entactin (HA Lm, 500 Pa) with a seeding density of 1000 cells/µL at 14 days (cell mask membrane stain (magenta) nuclei (grey) and SFTPC^{GFP+} expression (green), scale bar 100 µm).

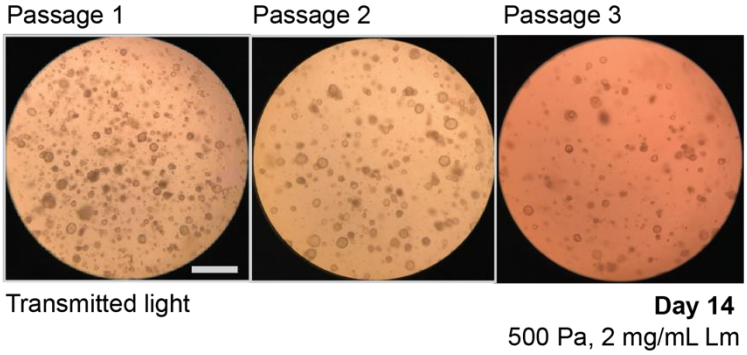

Supplementary Figure 3: Passaging of al alveolospheres in hyaluronic acid hydrogels with 2 mg/mL laminin/entactin
Representative images of alveolospheres after serial passages in hyaluronic acid hydrogels with 2 mg/mL laminin/entactin (HA Lm, 500 Pa, 1000 cells/µL).

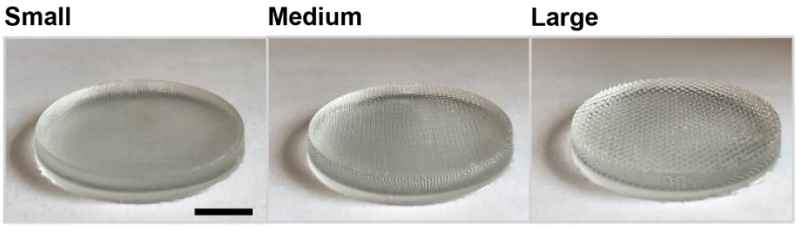

Supplementary Figure 4: Silicone replica molds made from EZSPHERES™ dishes
Representative images of silicone replica molds of different size that were fabricated from commercially available cell culture surfaces (EZSPHERES™, small: 200 µm/100 µm, medium: 500 µm/200 µm, large: 800 µm/300 µm (width/depth), scale bar 1 mm).

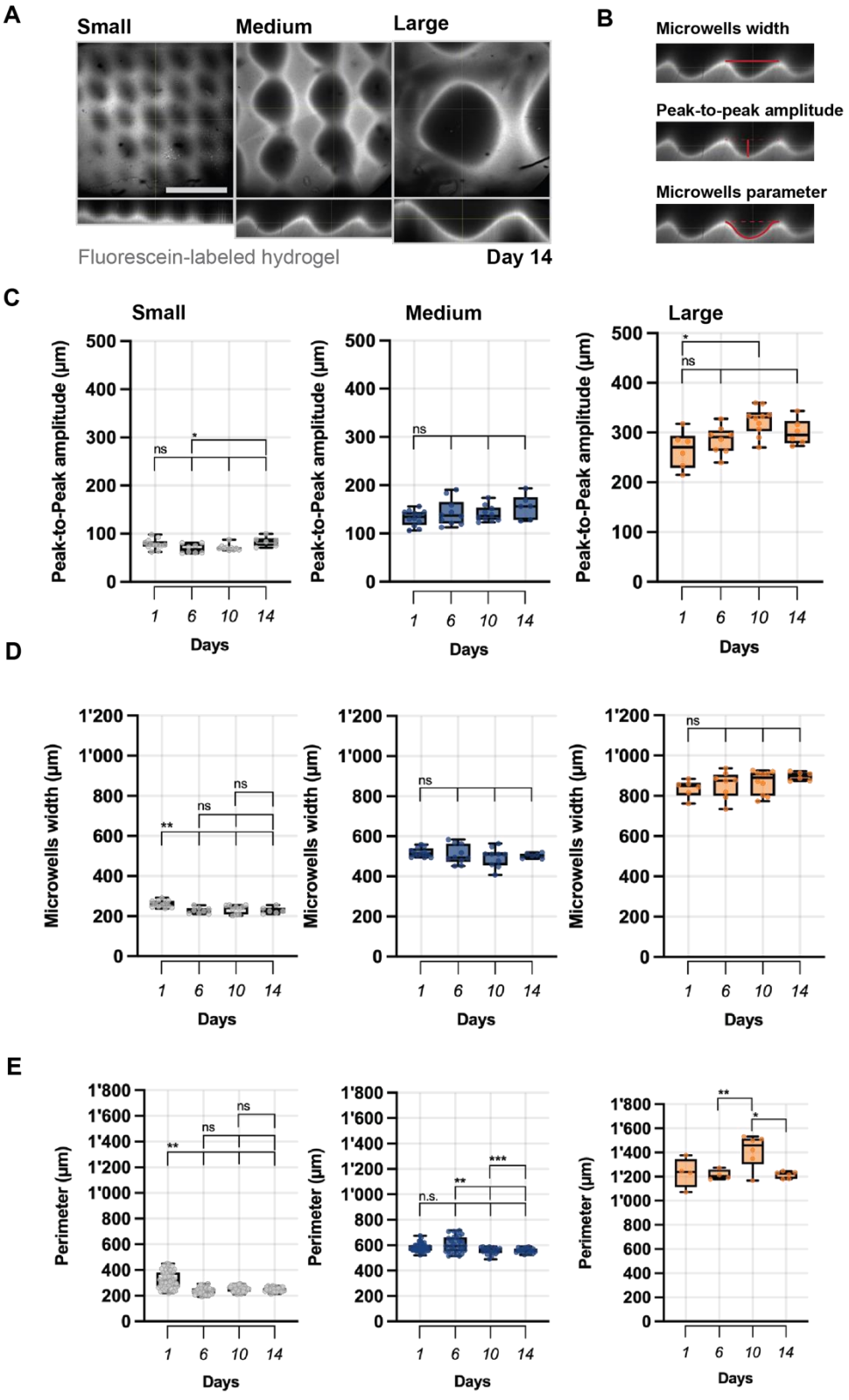

Supplementary Figure 5: Microwell hydrogel stability and fidelity
A Representative images of microwell hyaluronic acid hydrogels modified with fluoresceine and fabricated from silicone molds with different width and depth upon 14 days of swelling in saline (small: 200 µm/100 µm, medium: 500 µm/200 µm, large: 800 µm/300 µm (width/depth), scale bar 500 µm).

B Examples of ImageJ-based quantification of microwells width, peak-to-peak amplitude and microwells perimeter.
C Quantification of peak-to-peak amplitude of individual microwells during swelling in saline (day 1, 6, 10, 14), *p<0.05, ns = not significantly different by ANOVA and Bonferroni's multiple comparisons test, n = 11 (Small, Med) and n = 10 (Larg).
D Quantification of the width of individual microwells during swelling in saline (day 1, 6, 10, 14), **p<0.01, ns = not significantly different by ANOVA and Bonferroni's multiple comparisons test, n = 11 (Small, Med) and n = 10 (Larg).
E Quantification of the perimeter of individual microwells during swelling in saline (day 1, 6, 10, 14), **p<0.01, ns = not significantly different by ANOVA and Bonferroni's multiple comparisons test, n = 11 (Small, Med) and n = 10 (Larg).

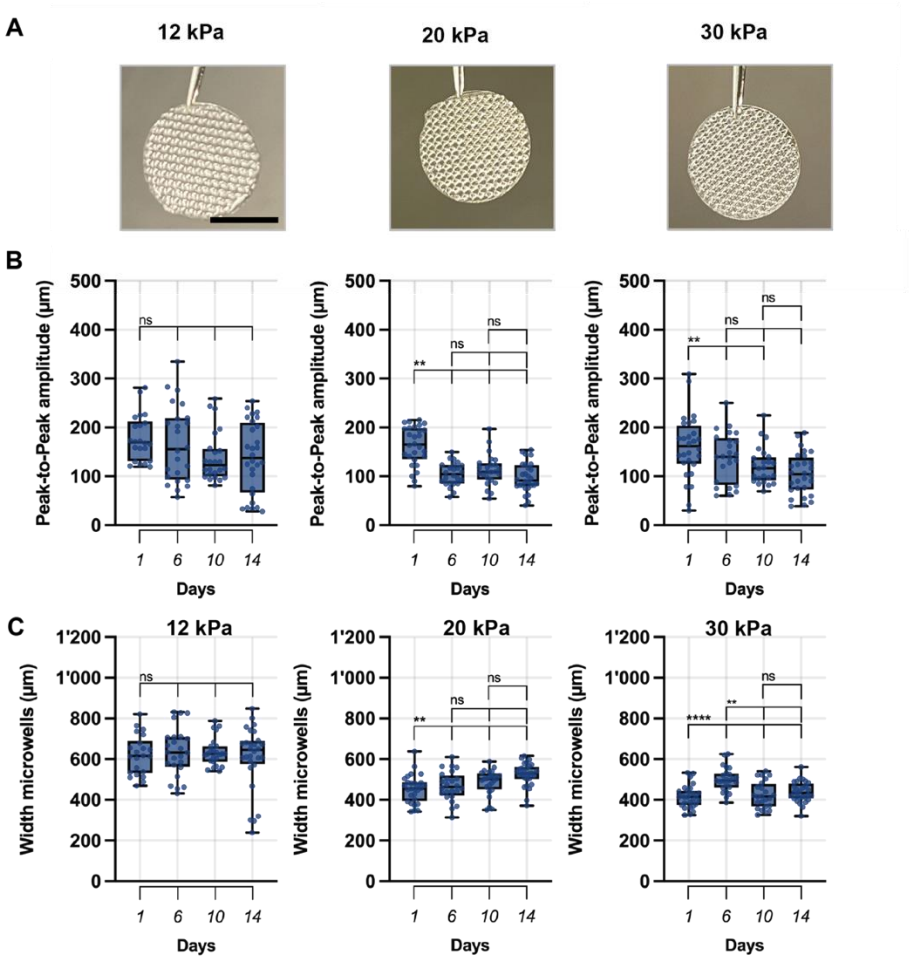

Supplementary Figure 6: Influence of initial elastic moduli on microwell hydrogel stability and fidelity
A Representative images of microwell hyaluronic acid hydrogels fabricated from silicone molds with different initial crosslinking densities widths upon 1 day of swelling in saline (12 kPa, 20 kPa and 30 kPa). **B** Quantification of peak-to-peak amplitude of individual microwells during swelling in saline (day 1, 6, 10, 14), **p<0.01, ns = not significantly different by ANOVA and Bonferroni's multiple comparisons test, n = 23 (12 kpa) and n = 26 (20 kPa, 30 kPa).
C Quantification of the width of individual microwells during swelling in saline (day 1, 6, 10, 14), **p<0.01, ****p<0.0001, ns = not significantly different by ANOVA and Bonferroni's multiple comparisons test, n = 23 (12 kpa) and n = 26 (20 kPa, 30 kPa).

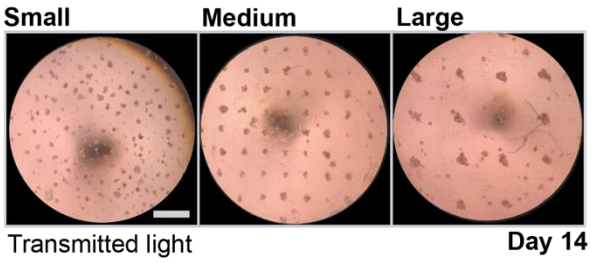

Supplementary Figure 7: Formation of alveolospheres in microwells of different size
Representative images of alveolospheres formed in microwells of different size at 14 days (small: 200 µm/100 µm, medium: 500 µm/200 µm, large: 800 µm/300 µm (width/depth), scale bar 1 mm).

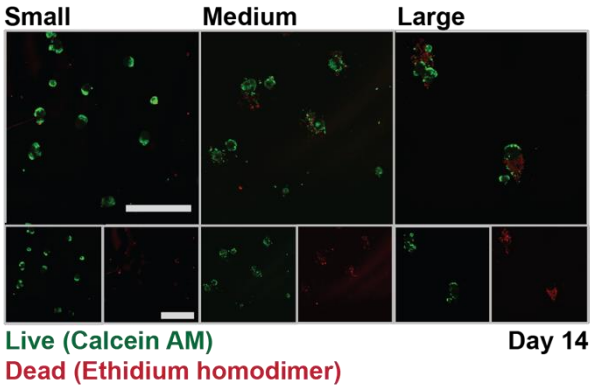

Supplementary Figure 8: Viability of alveolospheres within microwells of different size
Representative images of Calcein AM (live cells) and Ethidium homodimer (dead cells) staining of alveolospheres formed in microwells of different size at 14 days (small: 200 µm/100 µm, medium: 500 µm/200 µm, large: 800 µm/300 µm (width/depth), scale bars 500 µm).

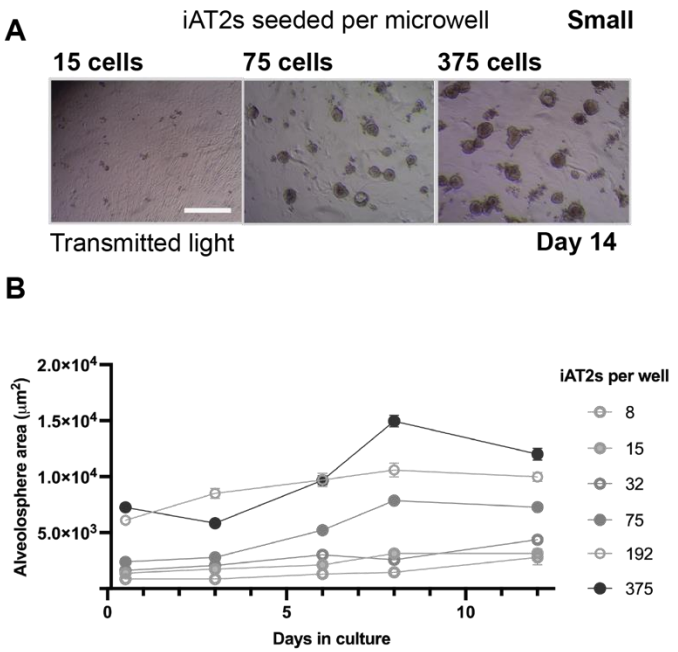

Supplementary Figure 9: Formation of alveolospheres in small microwells
A Representative images of alveolospheres formed from 15, 75 and 375 iAT2s per individual medium size microwell (200 µm/100µm width/depth) at 14 days of culture (scale bar 500 µm).
B Time course quantification of the projected area of alveolospheres formed from 8, 15, 32, 75, 192and 375 iAT2s over 14 days averaged from 3 independent experiments.

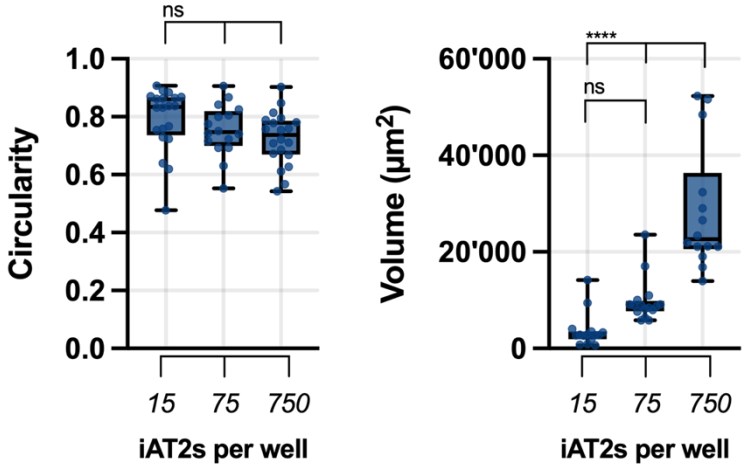

Supplementary Figure 10: Additional characterization of alveolospheres in medium microwells
Quantification of the circularity and volume of alveolospheres at 14 days in culture (****p<0.0001 by ANOVA and Bonferroni's multiple comparisons test, n = 30 (15 iAT2s), n = 16 (75 iAT2s), and n = 15 (750 iAT2s)).

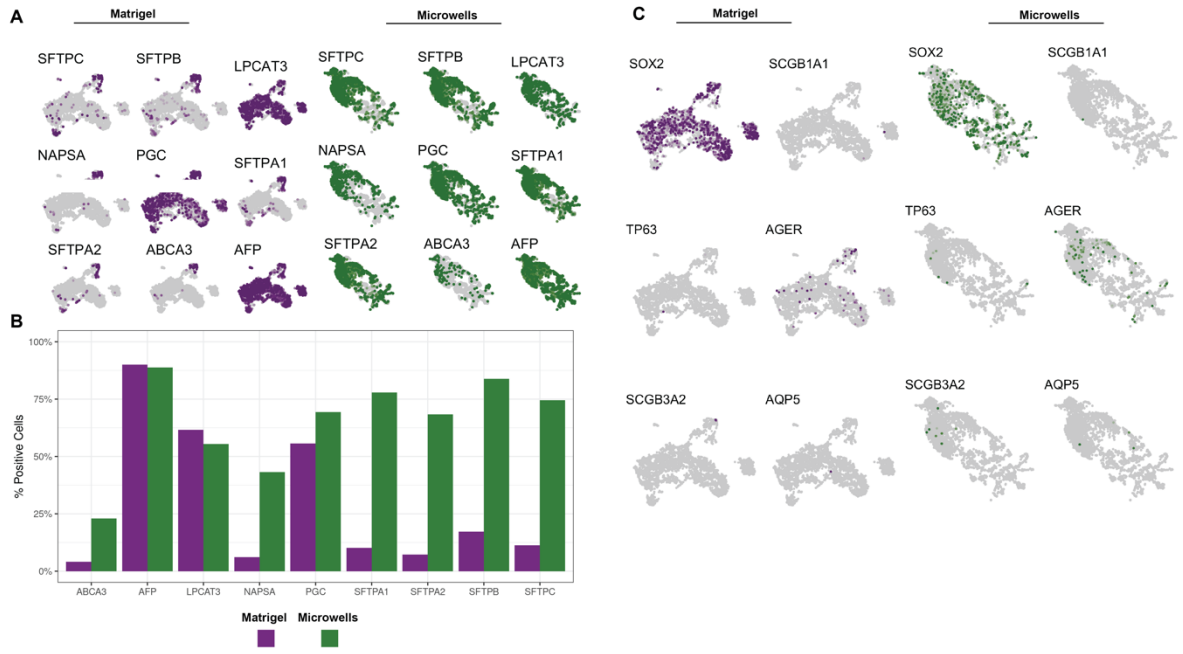

Supplementary Figure 11: ScRNA-seq characterization of alveolospheres
A UMAP representation and **B** gene expression proportion of AT-2 specific markers of cells within alveolospheres at 14 days cultured in Matrigel and atop microwells. **C** UMAP representation of markers of off-target cells within alveolospheres at 14 days cultured in Matrigel and atop microwells.

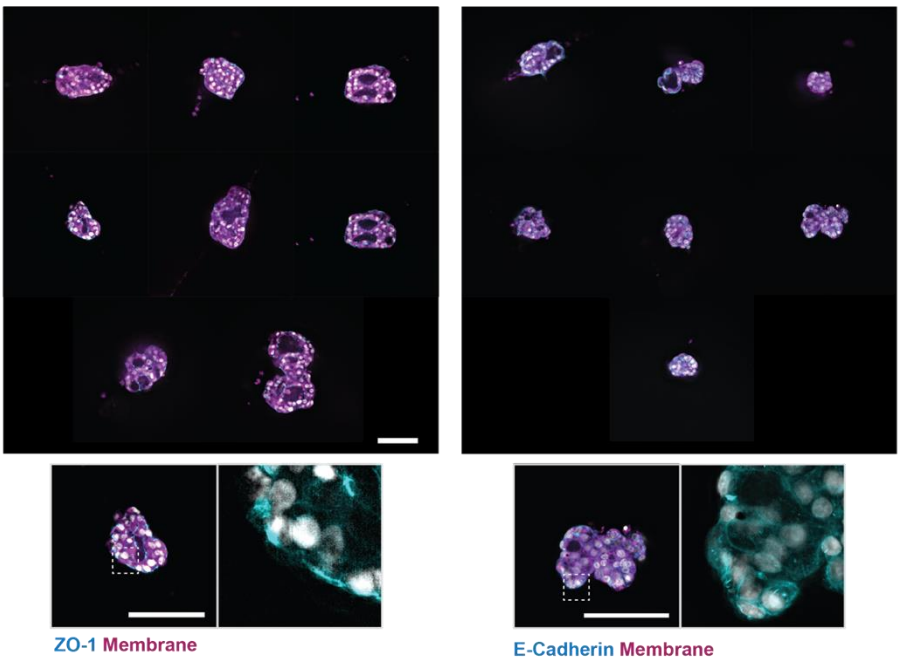

Supplementary Figure 12: Characterization of alveolosphere polarity
Representative images of **A** ZO-1 and **B** E-Cadherin expression in alveolospheres at 14 days of culture (cell mask membrane stain (magenta) nuclei (grey), and ZO-1/E-Cadherin (cyan), scale bars 100 µm).

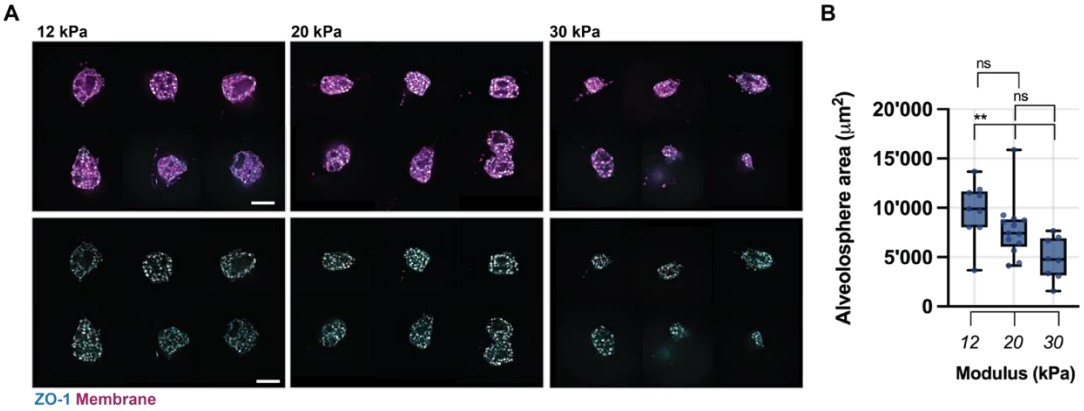

Supplementary Figure 13: Influence of initial elastic moduli on alveolosphere formation and polarity.
A Representative images of ZO-1 expression in alveolospheres at 14 days of culture in microwell hydrogels of 12 kPa, 20 kPa and 30 kPa elastic modulus (cell mask membrane stain (magenta) nuclei (grey), and ZO-1 (cyan), scale bars 100 µm) and B quantification of alveolosphere area at 14 days of culture in microwell hydrogels of 12 kPa, 20 kPa and 30 kPa elastic modulus ((**p<0.01 by ANOVA and Bonferroni's multiple comparisons test, n = 10 (12, 30 kPa), and n = 15 (20 kPa)).

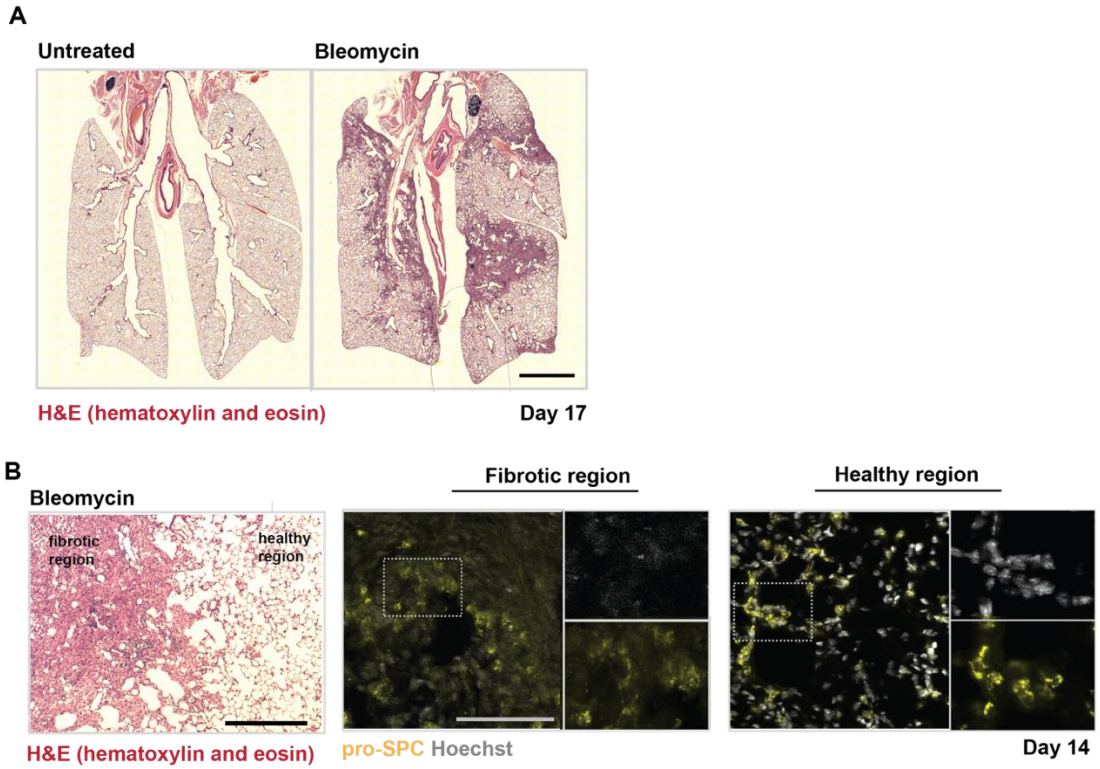

Supplementary Figure 14: Bleomycin injury of immunocompromised NOD SCID NSG gamma mice
A Representative images of hematoxylin and eosin (H&E) staining of fibrotic and healthy lungs of mice 17 days upon bleomycin injury (scale bar 2500 µm).
B Representative images of fibrotic and healthy regions (H&E, nuclei (grey) and pro-SPC (yellow), scale bars 500 µm (H&E), 100 µm (pro-SPC)).

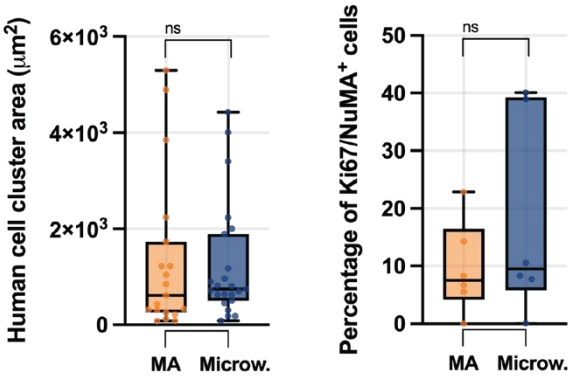

Supplementary Figure 15: Quantification of transplanted human cell areas
Quantification of the area and percentage of proliferating cells within transplanted human cell area at day 14 (ns = not significantly different by unpaired two-tailed *t*-test, averaged from 3 mice per group, n = 22 lung sections (Matrigel, area), n = 25 lung sections (microwells, area), n = 6 lung sections (Matrigel, microwells)).

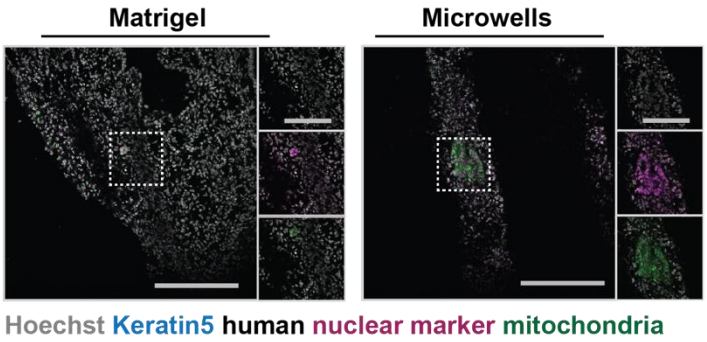

Supplementary Figure 16: Absence of dysplastic differentiation of human cells upon orthotopic transplantation
Representative images of Keratin 5 expression of transplanted human cells derived from alveolospheres upon culture in Matrigel or atop microwells (nuclei (grey), keratin 5 (cyan), human nuclear marker (magenta), and human mitochondrial marker (green), scale bars 100 µm).

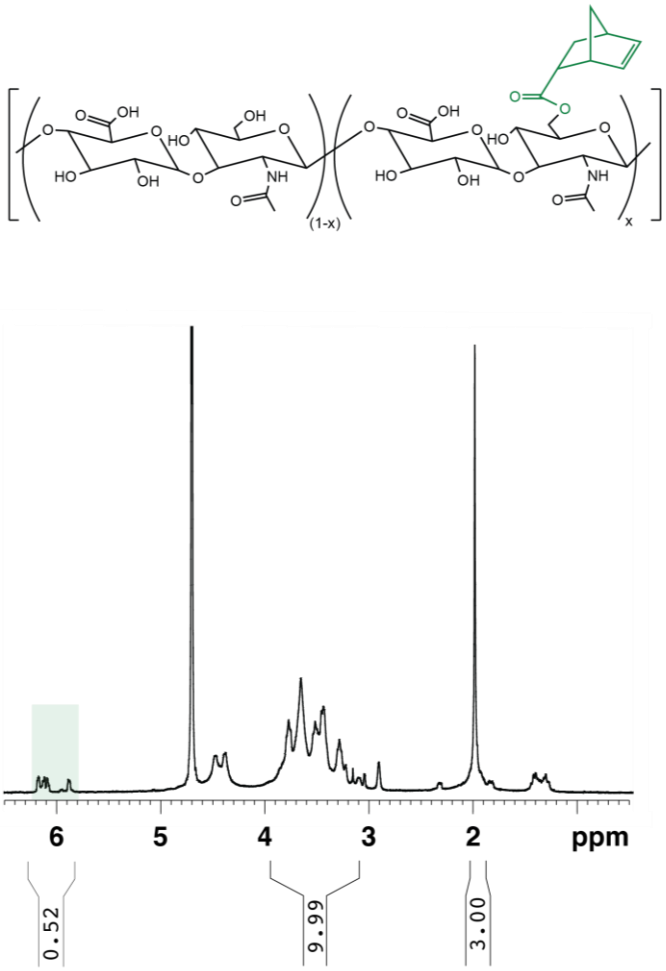

Supplementary Figure 17: ^{1}H NMR spectrum of norbornene-functionalized hyaluronic acid (NorHA) in D_2O. Modification of HA with norbornene (23%) determined by integration of vinyl protons (2H, shaded violet) relative to the sugar ring of HA (10H, shaded grey), analysis was done on each batch used to ensure consistency of modification.

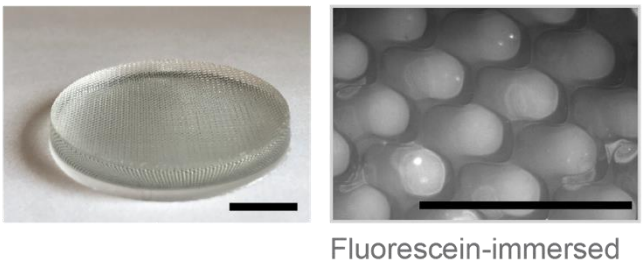

Supplementary Figure 18: Microstructure of silicone replica molds made from EZSPHERES™ dishes
Representative brightfield and fluorescent images of silicone replica molds fabricated from commercially available cell culture surfaces (EZSPHERES™, medium: 500 µm/200 µm (width/depth), scale bar 1 mm).